Energy Conversion and Management 294 (2023) 117567

Contents lists available at ScienceDirect

Energy Conversion and Management

journal homepage: www.elsevier.com/locate/enconman

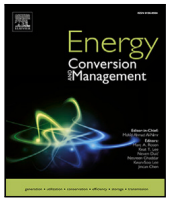

Mixed topology optimization: A self-guided boundary-independent approach for power sources

Mehrzad Alizadeh [a,*], Patcharawat Charoen-amornkitt [b], Takahiro Suzuki [a], Shohji Tsushima [a]

[a] Department of Mechanical Engineering, Graduate School of Engineering, Osaka University, Suita, 565-0871, Osaka, Japan
[b] Electrochemical Energy Storage and Conversion Laboratory, Department of Mechanical Engineering, Faculty of Engineering, King Mongkut's University of Technology Thonburi, Thung Khru, 10140, Bangkok, Thailand

ARTICLE INFO

Keywords:
Mixed optimization
Topology optimization
Electrochemical system
Power source

ABSTRACT

As the use of electrochemical devices becomes more prevalent, advanced optimization techniques, such as topology optimization, are being employed to improve their performance. Among various electrochemical systems, power sources have an intrinsic best operating point that corresponds to the maximum output power. This study proposes a mixed topology optimization approach to enhance the performance of these systems by a simultaneous modification of electrode structure and the working condition. In contrast to the conventional approaches, the proposed method focuses on enhancement of the maximum power point. Thanks to its self-guidance feature, this technique outperforms conventional topology optimization methods and eliminates the need for a prior decision on the optimization starting point. Therefore, the proposed approach has a significant potential for adapting the material distribution to the best working condition. The proposed approach enables more effective topological optimization and takes the utilization of topology optimization in power sources to the next level.

1. Introduction

The shift towards more sustainable resources [1–3] has led to a heightened emphasis on electrochemical technologies as an essential element in the envisioned societies of the future that rely on renewable energy [4]. Therefore, any improvement in the performance of these devices not only has significant implications for the sustainability of our energy systems and the reduction of greenhouse gas emissions but also holds the potential to improve human lives by enabling greater access to clean and reliable energy sources. Considering the pivotal role played by the microstructure of porous media in governing transport phenomena [5], the optimization of electrode composition has been extensively studied to enhance the performance of electrochemical devices such as batteries [6], fuel cells [7], and electrolyzers [8]. Parametric optimization, along with mathematical modeling, is commonly used to identify the best combination of constituents within an electrode. For instance, in a study of polymer electrolyte membrane fuel cells (PEMFCs) [9], researchers used mathematical optimization to identify the optimal platinum loading, platinum to carbon mass ratio (Pt/C), and ionomer to carbon ratio (I/C) with the aim of enhancing cell performance.

To broaden the capabilities of conventional parametric optimization, several studies [10,11] have proposed a so-called multi-domain or graded design. This approach entails partitioning the electrode domain into several sub-domains and independently optimizing the composition of each section to achieve a superior output in the final configuration. Recently, a more advanced mathematical tool known as topology optimization (TO) [12–14] has been utilized in a few research studies [15,16] to search for heterogeneous structures for electrodes of electrochemical devices. TO aims to find the optimal material distribution within a given design domain to optimize a specified objective (cost) function. Thanks to its higher degree of freedom compared to other optimization methods, TO enables the development of innovative designs with non-uniform shapes, which were previously unattainable through traditional parametric or shape optimizations. Roy and colleagues [15] employed TO to determine the optimal porosity distribution in electrodes of redox flow batteries. The optimization problem, aimed at minimizing electrode losses, was formulated as the total overpotential at a given current density. They conducted the optimization process at multiple current densities, resulting in different structures with varying objective function values. However, this study does not discuss the relative superiority of these designs. Deng and colleagues [16,17] integrated TO with an online machine learning technique to seek optimal topology for the porous electrode of a lithium-ion battery. Although they boosted the optimization algorithm

* Corresponding author.
E-mail address: alizadeh.mehrzad@gmail.com (M. Alizadeh).

https://doi.org/10.1016/j.enconman.2023.117567
Received 1 June 2023; Received in revised form 31 July 2023; Accepted 19 August 2023
Available online 31 August 2023

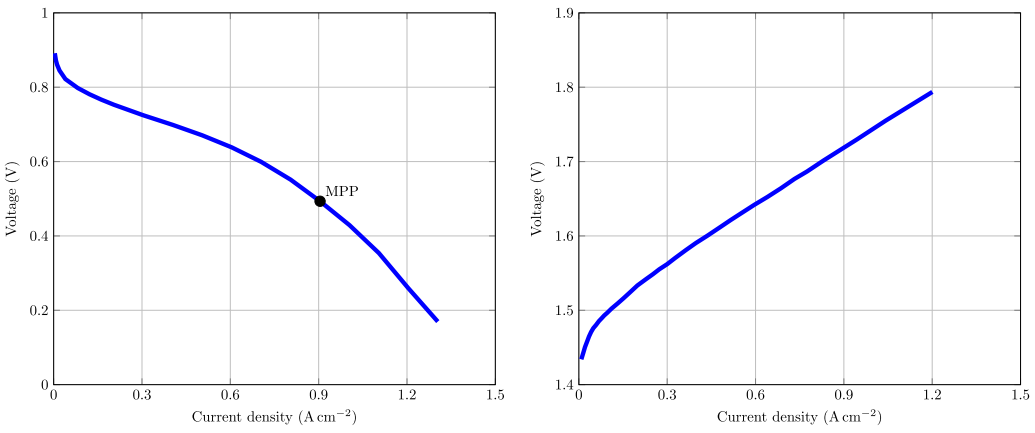

(a) PEMFC (b) PEMWE [18]

Fig. 1. Sample polarization curves of electrochemical (a) power source (PEMFC) and (b) power consuming (PEMWE) systems.

with a deep-learning technique, similar to what has been done in [15], these researchers maximized the specific energy of the battery during the discharge process at a fixed current density. In topological optimization of electrodes, researchers posed the problem in two different formulations, including: (1) minimizing overpotential at a fixed current density and (2) maximizing current density at a specified overpotential. While both strategies lead to a better performance in terms of power density, the two approaches produces distinct optimal heterogeneous layouts.

In any electrochemical device, the voltage and current density are interrelated, and their relationship is known as the polarization characteristic. This characteristic is a criterion for evaluating the performance of the device. For a specific device, once the value of either voltage or current density is known, the other one is automatically specified. The power density generated or consumed by an electrochemical device could be calculated by multiplying these two values. Fig. 1 provides sample polarization curves of a PEMFC and a polymer electrolyte membrane water electrolyzer (PEMWE) [18], representing electrochemical power source and power-consuming systems, respectively. TO can enhance the electrodes of both types of systems and consequently their performance by providing innovative structures. Minimization of overpotential at a specific current density leads into a vertical shift of polarization curve, and hence, we call it vertical optimization. Likewise, maximization of current density causes a horizontal shift in the polarization curve and therefore we refer to as horizontal optimization. This is what has been already addressed by previous researches [15,16]. However, what is missing in those studies is a mixed approach that is useful for power-generating systems. A mixed approach combines both vertical and horizontal methodologies to achieve a more comprehensive strategy. In any kind of power sources (e.g., fuel cells), the voltage and current density are negatively correlated, meaning that when a more current density is drawn, the voltage goes down (see Fig. 1(a)). This negative correlation gives a rise to a best operational point on the polarization curve of power sources where the power density is maximum. Given the fact that a power source is made to generate power, maximum power density point (MPP) might be used as a criterion for comparison between various designs. Electrochemical power-consuming systems (e.g., electrolyzers) have a positive correlation between voltage and current density (see Fig. 1(b)). In these systems, it is favorable to maximize the electrolysis rate while consuming minimum power density. If the minimum power density is assumed as the objective, a zero current density point (where the system is shut down) might be mistakenly considered as the best point. On the other hand, when the objective is changed to the highest possible electrolysis rate (i.e., the highest current density point), the consumed power density is the maximum. Therefore, unlike power sources, the polarization curve of these systems does not have any intrinsic best operating point in terms of power density.

The inherent difference between electrochemical power source and sink devices presents an opportunity for further improvement of power sources through a mixed optimization approach that considers both vertical and horizontal aspects To put it in other words, the results reported in previous research works [15,16] highly depend on the optimization approach (vertical or horizontal) and the point at which optimization is conducted. For instance, in a PEMFC that is working at a high working current density, the sluggish mass transport is the dominant mechanism. Hence, if a high current density point is selected together with a horizontal optimization, the algorithm favors only those design solutions that reduces the mass transport resistance. Similarly, if a vertical approach is chosen for optimization at a low current density point, at which the activation overpotential prevails, the algorithm prioritizes designs that decrease activation overpotential. Given the highly nonlinear nature of these systems, the MPP of an optimized structure cannot be guaranteed to be superior to that of the pre-optimized state. One may suggest that performing the optimization at a medium working condition may solve this problem. However, two challenges still remain: (1) exact selection of the medium working condition point and (2) selection between vertical and horizontal optimization approaches. Moreover, by performing either vertical or horizontal optimizations, the searching space on the polarization graph is confined only to a single line that passes the selected starting point. As a result, the algorithm may overlook other search spaces that might yield superior results. Finally, after performing the optimization with either vertical or horizontal approaches, it is necessary to plot the polarization curve for the optimized structure and to find MPP on the new characteristic curve.

In the present work, we propose a mixed topology optimization approach that resolves the aforementioned problems associated with the previous studies. This technique enhances the capacity of TO to optimize power sources, elevating it to a higher level. Prior research in the literature has solely benefited from the local-level design capabilities of TO. The proposed mixed topology optimization approach enhances the capacity of optimizing power sources by exploring optimal design solutions in a 2D polarization space, instead of limiting the optimization process to a single line. This is particularly important due to the highly nonlinear nature of electrochemical systems.

2. Methods

2.1. Formulation and algorithm

In the conventional horizontal or vertical TO of electrochemical systems, the objective function is defined as the minimization of total overpotential at a given current density (vertical optimization) or

maximization of current density at a given overpotential (horizontal optimization). Typically, the objective function is enhanced by updating the local volume fraction of constituents in an iterative procedure using a gradient-based algorithm, such as the well-known "globally convergent method of moving asymptotes" (GCMMA) algorithm [19]. Depending on the system of interest, the number of these constituents might be different. For instance, in Roy and colleagues' study [15] on optimizing the electrode structure of a redox flow battery, the authors utilized a porous media consisting of only two phases: solid and electrolyte. The summation of volume fractions of these two phases should be equal to unity at a local level. Therefore, controlling the volume fraction of one phase is enough for the optimization process, as the other volume fraction could be automatically calculated from the aforementioned equality constraint. In certain systems, such as the electrode of a fuel cell, multiple materials may be present. When dealing with optimization problems that involve multiple variables, any of these variables can be chosen as the decision variable, as long as the aforementioned equality constraint is met. Regardless of the number of design variables, the algorithm used in those studies could be summarized to the step-by-step procedure shown in Fig. 2(a). The optimization process starts with the initialization step in which the boundary conditions (B.C.) necessary for solving the governing equations are specified. To numerically simulate an electrochemical system, it is necessary to provide either the system voltage or current density in the form of B.C. as an input. Once either of these parameters is given, the other one could be determined by solving the system of governing equations. In fact, the B.C. prescribes the optimization point. In the subsequent steps, the sensitivity (gradient) of the objective function is calculated with respect to the design variables. Since the design variable is controlled locally, calculating the sensitivity using conventional methods, such as the finite difference forward method, is computationally expensive. To overcome this difficulty, an adjoint state method [20] is usually recruited, which is a computationally cheap technique. Unlike finite difference methods, which incur a higher computational cost as the number of decision variables increases, the adjoint method remains unaffected by the number of decision variables. Hence, it is particularly well-suited for topology optimization problems that involve a large number of decision variables. According to this approach, the total derivative of the objective function with respect to each decision variable can be expressed as follows:

$$\frac{dF_{\text{obj}}}{d\psi_{\text{i}}} = \frac{\partial F_{\text{obj}}}{\partial \psi_{\text{i}}} + \lambda^{\intercal}\frac{\partial \mathbf{G}_0}{\partial \psi_{\text{i}}} \tag{1}$$

where F_{obj} is objective function, ψ_{i} is decision variable i, λ is the vector of adjoint variables, and $\mathbf{G}$ is the system of governing equations. To evaluate the sensitivity, it is imperative to solve an additional single equation known as the adjoint equation, which is given as:

$$\left(\frac{\partial \mathbf{G}_0}{\partial \mathbf{U}}\right)^{\intercal}\lambda = -\left(\frac{\partial F_{\text{obj}}}{\partial \mathbf{U}}\right)^{\intercal} \tag{2}$$

where $\mathbf{U}$ is a vector of state variables. The process is followed by updating the design variables through an algorithm (e.g., GCMMA) and repeating the described procedure in a loop until the convergence is achieved. The GCMMA algorithm, employed in this study, extends the method of moving asymptotes (MMA) with guaranteed convergence. This iterative sequence involves solving the MMA-subproblem, followed by a subsequent line search. A comprehensive discussion of both MMA and GCMMA can be found in [19,21]. Furthermore, the convergence criterion employed in this study is based on the maximum number of iterations. A sufficiently large number of iterations is selected to ensure that the objective function remains stable and does not undergo significant changes.

In the proposed mixed approach, first, the problem formulation is changed to the maximization of the generated power. By alternating the voltage and current density, this approach aims to achieve the maximum power that is the multiplication of these two parameters. This might be translated as an increase or decrease in either voltage or current density. The distribution of constituents materials, $\boldsymbol{\psi}(\mathbf{x})$, should be changed in the given design domain, Ω, so that the objective function is maximized. The optimization problem is at least constrained by the system of governing equations ($\mathbf{G}_0 = 0$) and there might be N other additional constraints, $C_{\text{i}} \leq 0$ ($\text{i} = 1, \ldots, N$). With these explanations, the optimization problem reads as:

$$\begin{aligned} \max_{\boldsymbol{\psi}(\mathbf{x})} \quad & F_{\text{obj}} = P = I \times V \\ \text{s.t.} \quad & \mathbf{G}_0 = 0 \\ & C_{\text{i}} \leq 0 \quad \text{i} = 1, \ldots, N \end{aligned} \tag{3}$$

in which P, I, and V represent power density, current density, and voltage of the system, respectively. The complete procedure of the mixed TO is depicted in the flowchart of Fig. 2(b). In addition to the different choice of objective function compared to vertical/horizontal TO, the new approach updates the B.C. in each iteration. To accomplish this goal, the sensitivity (gradient) of the objective function should also be computed with respect to the B.C. in each iteration. Since the B.C. is only one variable, this sensitivity analysis may be conducted by a forward method. Next, the B.C. should be updated based on the measured gradient using a mathematical algorithm, such as the method of steepest descent. The updated B.C. will be feedbacked to the governing equation solver to be used for solving the system in the next iteration. The process is repeated until the convergence criteria are met. The algorithm is no longer limited to searching the polarization space along a single vertical or horizontal direction. As a result, it is now free to explore any direction it chooses, greatly expanding the scope of the optimization process. By updating the B.C. in the optimization loop, the proposed strategy becomes self-guided in searching the entire polarization curve and find superior design solutions to those achieved by conventional TO. This means that irrespective of the initial B.C. (optimization starting point), the optimization will always result in the same value of the objective function. Moreover, it is assured that this value corresponds to the MPP of the new design solution. Hence, there is no need for an additional step to look for MPP of the new structure.

2.2. Triple-phase electrochemical reaction–diffusion system

The mixed TO is applied to a triple-phase electrochemical reaction–diffusion (ERD) system. Such a system is analogous to the catalyst layer of a PEMFC. However, it does not represent all the phenomena that are taking place in an electrode of a fuel cell. It is noteworthy that this arbitrary case study is conducted to demonstrate the superiority of mixed topology optimization compared to the two conventional approaches (horizontal and vertical). Nevertheless, the strategy we have introduced can be applied to any real system that involves optimizing parameters with negative correlation. The ERD system is a porous reactor consisting of three phases, including an electrolyte phase, a solid phase, and pores as shown in Fig. 3. The first two phases are responsible for the transport of ions and electrons, respectively. A reactant is diffused into the system through the pores while getting reduced through a catalytic reaction as follows:

$$\text{A}^{\text{Ox}} + n\text{e}^{-} \longrightarrow \text{A}^{\text{Red}} \tag{4}$$

where A^{Ox} and A^{Red} are oxidizing and reduced agents, respectively, and e^{-} denotes the electron. The coefficient n is the number of exchanged electrons in this redox reaction. The polarization characteristics of this system are controlled by three mechanisms, including activation, Ohmic, and concentration limitations. The electric charges and mass transport are described by Ohm law and Fick's second law of diffusion, respectively. Moreover, the transport and catalytic properties are correlated to the volume fractions of each phase through a power-law.

The conservation of species, ion, and electron are expressed in a non-dimensional form as:

$$\nabla^{*} \cdot \left(\theta_1 \varepsilon_3^{\beta_1} \nabla^{*} C^{*}\right) + \varepsilon_2^{\beta_4} j_{\text{src}}^{*} = 0 \tag{5}$$

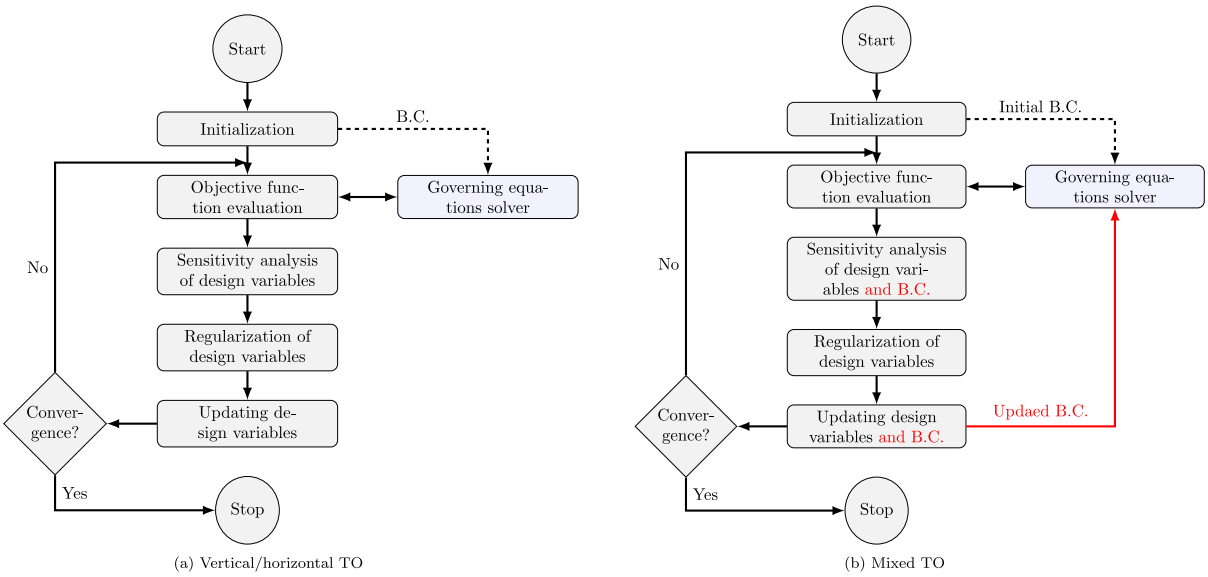

Fig. 2. Flow chart of optimization algorithm (a) conventional vertical/horizontal TO (b) mixed TO.

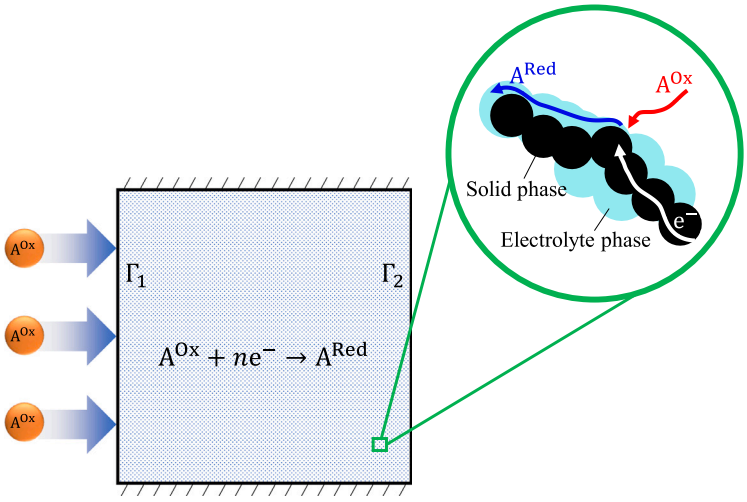

Fig. 3. Schematic of triple-phase ERD system.

$$\nabla^* \cdot \left(\frac{\theta_2}{1+\theta_3} \varepsilon_1^{\beta_2} \nabla^* \phi_l^* \right) + \varepsilon_2^{\beta_4} j_{src}^* = 0 \tag{6}$$

$$\nabla^* \cdot \left(\frac{\theta_2 \theta_3}{1+\theta_3} \varepsilon_2^{\beta_3} \nabla^* \phi_s^* \right) - \varepsilon_2^{\beta_4} j_{src}^* = 0 \tag{7}$$

where C^*, ϕ_l^*, and ϕ_s^* are concentration of reactant, electrolyte phase potential, and solid phase potential, respectively. ε_1 to ε_3 are representing volume fraction of ionomer phase, solid phase, and voids, respectively. Moreover, j_{src}^* is the current density source and β_1 to β_4 are penalty exponents for mass diffusion, ion transport, electron transport, and electrochemical surface area, respectively. The terms ε^β dictate how effective transport properties (diffusivity and conductivities) and rate properties (electrochemical surface area) are controlled by the volume fraction of constituents. ∇^* denotes differentiation with respect to dimensionless coordinates. The current density source is determined by the renowned Butler-Volmer kinetics after non-dimensionalization by the exchange current density of the system as follows:

$$j_{src}^* = -C^* \exp\left(-\alpha \eta^*\right) \tag{8}$$

in which α is charge transfer coefficient and η^* is the dimensionless overpotential. The overpotential, η, is converted to a dimensionless form with reference to the characteristic potential $\phi_0 = \frac{RT}{F}$. T, R, and F are system temperature, universal gas constant, and Faraday constant, respectively. The dimensionless groups, θ_1 to θ_3 in the governing Eqs. (5) to (7) are defined as:

$$\begin{aligned} \theta_1 &= \frac{D^0}{L^2 a^0 i_0/(C_0 F)} \\ \theta_2 &= \frac{(\sigma_l^0 + \sigma_s^0)}{L^2 a^0 i_0/\phi_0} \\ \theta_3 &= \frac{\sigma_s^0}{\sigma_l^0} \end{aligned} \tag{9}$$

where D^0, σ_l^0, σ_s^0, a^0, and i_0 are bulk mass diffusivity, ionic conductivity, electric conductivity, electrochemical surface area, and exchange current density, respectively. Also, L is the characteristic length of the system and C_0 is the reference concentration. The dimensionless numbers establish the correlation between various system characteristics and materials properties. To solve the governing equations, a set of boundary conditions (B.C.s) is required. The choice of B.C.s depends on the optimization strategy of interest (vertical, horizontal, or mixed optimization). However, some considerations are employed to

obtain a fair comparison between various optimization strategies. In a vertical optimization, the objective is to increase the voltage (decrease the overpotential) of the system at a given current density. However, horizontal optimization aims to increase the current density of the system at a prescribed voltage level. In either case, the concentration of reactant species is fixed on boundary Γ_1 ($C^*|_{\Gamma_1} = C^*_{\text{bnd}}$) and other boundaries are isolated to any mass flux. Moreover, electrons are only allowed to pass through Γ_1 and ions are allowed to only pass Γ_2. In a vertical approach, the system current density is predetermined as a problem input by fixing the electrolyte current density on boundary Γ_1 ($I^*_l|_{\Gamma_2} = I_{\text{bnd}}$) and fixing the ϕ^*_s on boundary Γ_1 ($\phi^*_s|_{\Gamma_1} = \phi^*_{s,\text{bnd}}$). Having these B.C.s, the solution of the governing equation would give the electrolyte potential on the boundary Γ_2. The cell voltage is defined as $V^* = \phi^*_s|_{\Gamma_1} - \phi^*_l|_{\Gamma_2}$. For a fixed current density, I_{bnd}, a better design solution should increase the system voltage (V^*). In a horizontal approach, however, the system voltage is predetermined as a problem input by fixing $\phi^*_s|_{\Gamma_1} = \phi^*_{s,\text{bnd}}$ on Γ_1 and $\phi^*_l|_{\Gamma_2} = \phi^*_{l,\text{bnd}}$ on Γ_2. The system voltage under such a setting is determined as $V^* = \phi^*_s|_{\Gamma_1} - \phi^*_l|_{\Gamma_2}$, which is constant. Having a constant voltage, the solution of governing equations would result in the system's current density. In this approach, the aim is to increase the current density. As a result, a topologically optimized layout should provide a higher current density. To ensure a fair comparison between different strategies, two considerations are included. First, in all optimizations, the common fixed concentration is used on the boundary Γ_1. Moreover, the starting point of all optimizations is the same. Since mixed TO is independent of B.C., picking either of voltage or current density as a B.C. and computing the other as a solution of the governing equations does not impact the results.

2.3. Simulation and implementation

The numerical simulation and optimization are performed using COMSOL Multiphysics® (version 5.6). The system of governing equations is solved using the finite element method (FEM) in a 1×1 dimensionless square domain (see Fig. 3). The number of meshes in all simulations is kept to be 10000. The same grids used for FEM simulation are used in the optimization process as decision variables. During the optimization process, the design variables are allowed to change between $0 \leq \varepsilon_1 \,\&\, \varepsilon_2 \leq 0.5$ in each mesh. This means that the other volume fraction could alternate between zero and one ($0 \leq \varepsilon_3 \leq 1$). For vertical and horizontal optimizations, the objective functions are set out to be overpotential (at a given current density) and current density (at a given voltage), respectively. For the mixed TO, the objective function is defined as power density according to Eq. (3). The sensitivity of objective function with respect to the volume fractions is calculated using the adjoint method. In addition, the gradient of F_{obj} with respect to the B.C. is evaluated using a forward method. In all optimizations, the design solutions are smoothed using a Helmholtz filter [22] and hyperbolic tangent project [23]. These regularization measures prevent checkerboard pattern in the optimal structure, which is a well-studied problem in TO [24].

3. Results and discussions

The mixed TO optimization is performed on the triple-phase ERD system described in Section 2. The objective is to maximize the power density produced by the system by controlling the distribution of volume fractions of each phase under the following constraint:

$$\varepsilon_1 + \varepsilon_2 + \varepsilon_3 = 1 \tag{10}$$

The constraint expressed in Eq. (10) is a physical constraint coming from the fact that at each position, the summation of volume fractions of all phases should be unity. Thus, two of these volume fractions could be considered as design variables and the third one is computed from the constraint. Furthermore, an inequality constraint is taken into account for the two design variables in the following form.

$$\varepsilon_{\min} \leq \varepsilon_1 \text{ and } \varepsilon_2 \leq \varepsilon_{\max} \tag{11}$$

where $\varepsilon_{\min}$ and $\varepsilon_{\max}$ represent the lower and upper bounds of the design variables, respectively. For the specific case study discussed in this paper, it is assumed that $\varepsilon_{\min} = 0$ and $\varepsilon_{\max} = 0.5$. As mentioned before, the transport and rate properties are related to the volume fraction of constituents. A proper distribution of volume fractions should result in a better performance (higher power density) owing to a compromise between various processes. The dimensionless characteristics of the system for all optimization scenarios are: $\theta_1 = 1$, $\theta_2 = 50$, and $\theta_3 = 5$. Also, the dimensionless concentration on the boundary is set to be $C^*_{\text{bnd}} = 1$. Since the two other boundary conditions (system voltage or current density) are linked, the correlation is shown for a range of these parameters as a polarization curve in Fig. 4(a).

For the sake of simplicity, the results reported in this section are non-dimensionalized using proper references points. As a benchmark, the conventional vertical and horizontal TO are used to optimize the system. The initial layout for all optimizations is a uniform distribution of volume fractions given by $\varepsilon_1 = \varepsilon_2 = 0.25$ and $\varepsilon_3 = 0.5$. For comparison between vertical, horizontal, and mixed approaches, a common starting point ($I^* = 4.51$ and $V^* = 8$) on the polarization curve of the system before optimization is chosen (see Fig. 4(a)). It is noteworthy that the asterisk sign denotes the dimensionless parameters. In order to ensure a fair comparison, the inlet concentration of the reactant has been kept fixed and equal across all optimization runs. It will be shown later that the mixed optimization is independent of this starting point. Figs. 4(a) and 4(b) illustrate the polarization and power density curves of the system before and after optimization. Upon comparison of MPP, it becomes clear that the mixed optimization outperforms the other two strategies. When using a horizontal optimization algorithm, the focus is on structural designs that improve current density. As current density increases, mass transport limitations become more significant, and the algorithm takes this into account. Consequently, as shown in Figs. 4(a) and 4(b), the layout obtained through a horizontal approach performs better in high current density regions than one obtained through vertical optimization. Mixed optimization aims to improve power density by simultaneously controlling both the layout and working conditions of a system. Unlike conventional approaches that prioritize either current density or voltage, mixed optimization seeks to enhance their combined effect (i.e., power density). As a result, this approach provides a superior MPP compared to the other two methods. To further expand on the discussion, horizontal optimization was carried out from a different starting point (i.e., $I^* = 14.95$ and $V^* = 1.5$). A comparison between the results of horizontal optimization from the two different starting points reveals two distinct outcomes. Figs. 4(a) and 4(b) illustrate that conducting the horizontal optimization at V^*=1.5 leads to a structural design that outperforms the mixed TO approach at high current densities ($I > 19.5$). However, this higher current density is achieved at a low voltage level, which is unfavorable. On the other hand, in regions of low current density and in terms of MPP, the mixed TO approach provides a superior design. When performing horizontal optimization with a starting point in a low voltage region (high current density), the algorithm focuses on improving the dominant loss mechanism, which is mass transport limitation. This is achieved by increasing the porosity through the formation of numerous large diffusion channels. Consequently, the resulting layout does not exhibit good performance at low current density, where an enhanced distribution of solid material is crucial. Nevertheless, the mixed TO approach overcomes this challenge by adjusting the layout and working conditions simultaneously. This enables the attainment of the highest possible MPP through the mixed approach. The optimized layout obtained from mixed TO is shown in Figs. 4(c) to 4(e). It can be seen that the optimal distribution of materials within the design domain leads to a complex tree-root-like structure. The diffusion channels formed by high concentration of voids

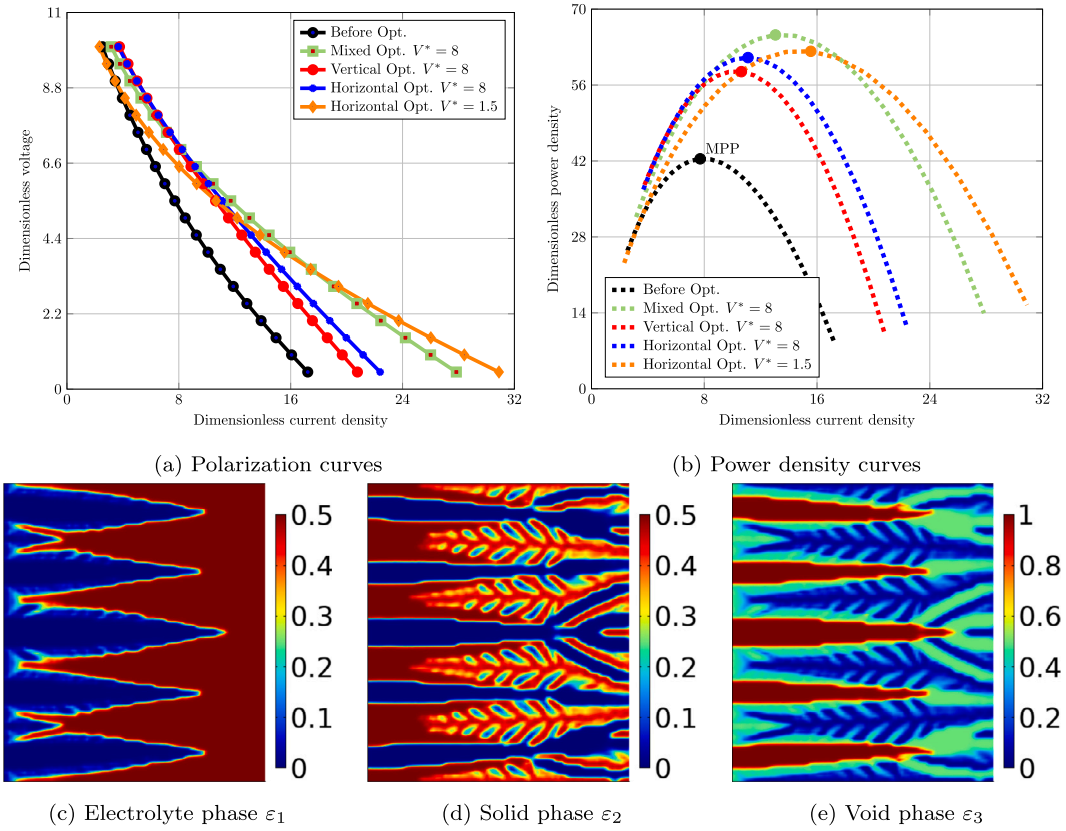

(a) Polarization curves (b) Power density curves

(c) Electrolyte phase ε_1 (d) Solid phase ε_2 (e) Void phase ε_3

Fig. 4. (a) Polarization curves and (b) power density curves of system before and after optimization; The optimal volume fraction distribution of (c) electrolyte, (d) solid, and (e) void phases using mixed TO.

at some parts of the systems (Fig. 4(e)) facilitate delivery of reactant material over the entire system. In nature, such a vascular layout might be seen in the leaf of plants. The network of veins that transport water and nutrients throughout a leaf exhibits a similar structural pattern. Likewise, the heterogeneous distributions of electrolyte and solid phases (Figs. 4(c) and 4(d)) improve the transport of ions and electrons, which in return enhances the overall system performance.

In order to demonstrate the boundary condition-independence and self-guidance of mixed TO, the optimization process was carried out with four distinct starting points. The resulting optimization paths and convergence history for all four cases can be observed in Fig. 5. Each path in Fig. 5(a) shows how the polarization points changes in every optimization iteration. What stands out in this figure is that regardless of the starting point (i.e., initial B.C.), all optimization runs converged to the same final point. This final point corresponds to MPP of the optimized layout. Hence, the new mixed approach is boundary-independent. Moreover, these findings also demonstrate that the proposed technique is not confined to searching on a single horizontal or vertical line. Instead, the algorithm is now free and can explore any direction it chooses. As a result, the proposed technique is self-guided. In conventional TO, the algorithm only improved the layout for a specific working condition. However, the mixed approach simultaneously looks for the best working condition and system layout. This enables the algorithm to automatically adapt the layout to changes in the working condition, leading to better outputs. As depicted in Fig. 5(b), the initial objective function value and the convergence history of each optimization vary due to the different starting points. Nevertheless, the convergence plots confirm that the utilization of mixed TO ensures that all optimizations ultimately converge to the same objective function value. Furthermore, as previously mentioned, the maximum number of iterations serves as the convergence criterion for all optimizations in this study. Notably, the selected number proves sufficient to achieve a stable convergence, where the objective function remains unchanged after approximately 100 iterations.

4. Conclusion

TO is shown to have a great potential for improving the performance of electrochemical devices by generating innovative structure for the electrodes. Despite its significant capability in enhancing electrode structure, the application of this optimization tool has remained limited to simple vertical or horizontal approaches. Here a new approach in implementation of TO for power sources called “mixed topology optimization” is presented. Compared to the traditional vertical or horizontal TO that look for an optimal material distribution on a single line in the polarization plane, the proposed mixed TO extends the search space to the entire polarization plane. This expansion in the search space is obtained at a small computational cost of a gradient calculation using the forward method only for B.C. (one variable). Considering the nonlinear nature of the electrochemical system, this additional step escalates the capability of TO. Of greater consequence, however, is the self-guidance and B.C.-independence of the proposed method. With the mixed TO, the optimization will reach the highest possible power with no concern regarding the impact of the starting point on the outcome. The proposed approach is tested on a triple-phase ERD system in which an electrochemical redox reaction is generating power. It is shown that the mixed TO outperforms conventional vertical and horizontal optimizations. Moreover, it is tested under various starting points and the output is always the same. This proves that the proposed method is independent of the starting point. This feature makes the users free of any prior decision before starting the optimization process. The development of a B.C.-independent approach that can outperform

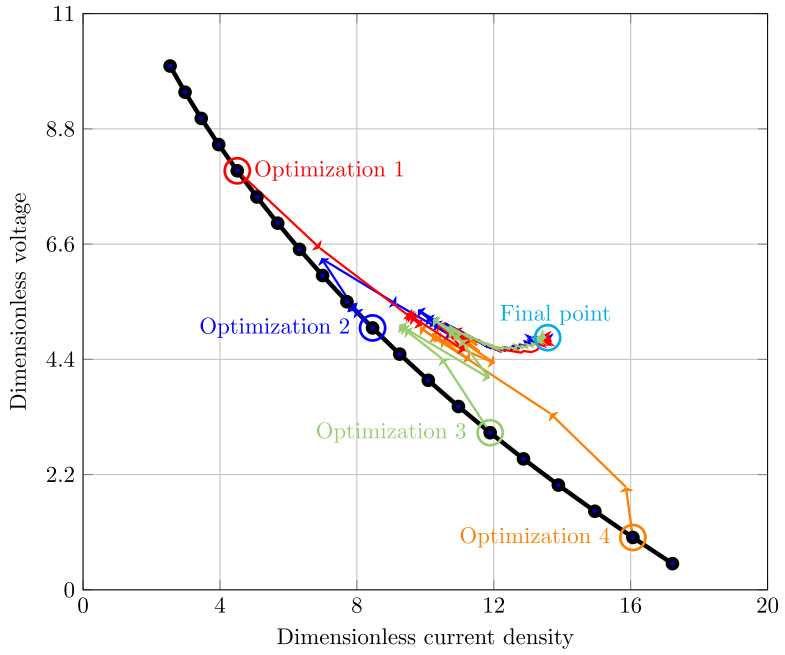

(a) Optimization paths of four mixed TO with various starting points

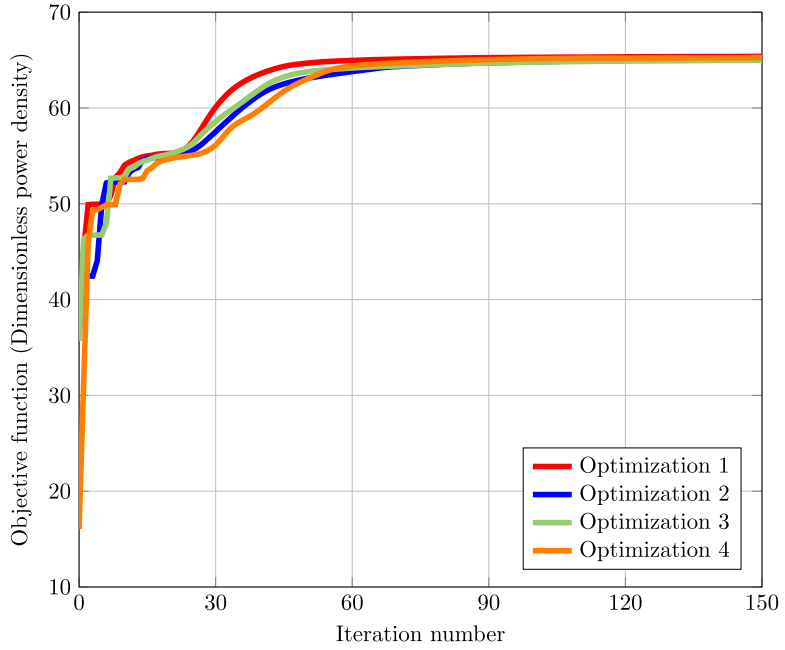

(b) Power density curves

Fig. 5. Optimization paths of four mixed TO with various starting points.

conventional techniques represents a promising step forward in the optimization of power sources. This approach provides a powerful tool that was not available before, enabling more effective optimization and ultimately improving the performance of power sources.

CRediT authorship contribution statement

Mehrzad Alizadeh: Conceptualization, Methodology, Software, Formal analysis, Investigation, Writing – original draft, Visualization. **Patcharawat Charoen-amornkitt:** Software, Formal analysis, Investigation, Writing – review & editing, Visualization. **Takahiro Suzuki:** Formal analysis, Data curation. **Shohji Tsushima:** Conceptualization, Formal analysis, Writing – review & editing, Supervision.

Declaration of competing interest

The authors declare the following financial interests/personal relationships which may be considered as potential competing interests: Mehrzad Alizadeh reports financial support was provided by Japan Society for the Promotion of Science. Shohji Tsushima reports financial support was provided by Japan Society for the Promotion of Science. Patcharawat Charoen-amornkitt reports financial support was provided by the Asahi Glass Foundation.

Data availability

No data was used for the research described in the article.

Acknowledgments

This work was supported by Grant-in-Aid for JSPS Fellows number 22KJ2198, JSPS KAKENHI Grant number 21H04540, and the Asahi Glass Foundation.

References

[1] Nantasaksiri K, Charoen-amornkitt P, Machimura T. Integration of multicriteria decision analysis and geographic information system for site suitability assessment of napier grass-based biogas power plant in southern thailand. Renew. Sustain. Energy Transit. 2021;1:100011. http://dx.doi.org/10.1016/j.rset.2021.100011.

[2] Nantasaksiri K, Charoen-amornkitt P, Machimura T, Hayashi K. Multi-disciplinary assessment of napier grass plantation on local energetic, environmental and socioeconomic industries: A watershed-scale study in southern thailand. Sustainability 2021;13(24):13520. http://dx.doi.org/10.3390/su132413520.

[3] Nantasaksiri K, Charoen-Amornkitt P, Machimura T. Land potential assessment of napier grass plantation for power generation in thailand using SWAT model. Model validation and parameter calibration. Energies 2021;14(5):1326. http://dx.doi.org/10.3390/en14051326.

[4] Matsui Y, Kawase M, Suzuki T, Tsushima S. Electrochemical cell recharging by solvent separation and transfer processes. Sci Rep 2022;12(1):3739. http://dx.doi.org/10.1038/s41598-022-07573-x.

[5] Wang Z, Lai B, Wang H, Xiao H, Ming P. Effects of micropore characteristics in the metal skeleton on heat and mass transfer in an open foam structure for thermal management in the hydrogen UAV. Int J Therm Sci 2022;179:107628. http://dx.doi.org/10.1016/j.ijthermalsci.2022.107628.

[6] Huang Y, Zhao L, Li L, Xie M, Wu F, Chen R. Electrolytes and electrolyte/electrode interfaces in sodium-ion batteries: from scientific research to practical application. Adv Mater 2019;31(21):1808393. http://dx.doi.org/10.1002/adma.201808393.

[7] Xing L, Shi W, Su H, Xu Q, Das PK, Mao B, Scott K. Membrane electrode assemblies for PEM fuel cells: A review of functional graded design and optimization. Energy 2019;177:445–64. http://dx.doi.org/10.1016/j.energy.2019.04.084.

[8] Bühler M, Hegge F, Holzapfel P, Bierling M, Suermann M, Vierrath S, Thiele S. Optimization of anodic porous transport electrodes for proton exchange membrane water electrolyzers. J Mater Chem A 2019;7(47):26984–95. http://dx.doi.org/10.1039/C9TA08396K.

[9] He P, Mu Y-T, Park JW, Tao W-Q. Modeling of the effects of cathode catalyst layer design parameters on performance of polymer electrolyte membrane fuel cell. Appl Energy 2020;277:115555. http://dx.doi.org/10.1016/j.apenergy.2020.115555.

[10] Li W, Lin R, Yang Y. Investigation on the reaction area of PEMFC at different position in multiple catalyst layer. Electrochim Acta 2019;302:241–8. http://dx.doi.org/10.1016/j.electacta.2019.02.003.

[11] Chen G-Y, Wang C, Lei Y-J, Zhang J, Mao Z, Mao Z-Q, Guo J-W, Li J, Ouyang M. Gradient design of pt/c ratio and nafion content in cathode catalyst layer of PEMFCs. Int J Hydrogen Energy 2017;42(50):29960–5. http://dx.doi.org/10.1016/j.ijhydene.2017.06.229.

[12] Charoen-amornkitt P, Alizadeh M, Suzuki T, Tsushima S. Entropy generation analysis during adjoint variable-based topology optimization of porous reaction-diffusion systems under various design dimensionalities. Int J Heat Mass Transfer 2023;202:123725. http://dx.doi.org/10.1016/j.ijheatmasstransfer.2022.123725.

[13] Lin TY, Baker SE, Duoss EB, Beck VA. Topology optimization of 3D flow fields for flow batteries. J Electrochem Soc 2022;169(5):050540. http://dx.doi.org/10.1149/1945-7111/ac716d.

[14] Wang Z, Wang H, Xiao H, Bai J, Zhao X, Wang S. Enhancing heat dissipation and mass transfer of oxygen gas flow channel in a proton exchange membrane fuel cell using multiobjective topology optimization. Int J Hydrogen Energy 2023. http://dx.doi.org/10.1016/j.ijhydene.2023.05.023.

[15] Roy T, Salazar de Troya MA, Worsley MA, Beck VA. Topology optimization for the design of porous electrodes. Struct Multidiscip Optim 2022;65(6):171. http://dx.doi.org/10.1007/s00158-022-03249-2.

[16] Deng C, Lu W. Geometry optimization of porous electrode for lithium-ion batteries. Ecs Trans. 2020;97(7):249. http://dx.doi.org/10.1149/09707.0249ecst.

[17] Deng C, Wang Y, Qin C, Fu Y, Lu W. Self-directed online machine learning for topology optimization. Nat. Commun. 2022;13(1):388. http://dx.doi.org/10.1038/s41467-021-27713-7.

[18] van Der Merwe J, Uren K, van Schoor G, Bessarabov D. Characterisation tools development for PEM electrolysers. Int J Hydrogen Energy 2014;39(26):14212–21. http://dx.doi.org/10.1016/j.ijhydene.2014.02.096.

[19] Zillober C. A globally convergent version of the method of moving asymptotes. Struct. Optim. 1993;6(3):166–74. http://dx.doi.org/10.1007/BF01743509.

[20] Antil H, Kouri D, Lacasse M, Ridzal D. Frontiers in PDE-Constrained Optimization. The IMA Volumes in Mathematics and its Applications, New York: Springer; 2018.

[21] Svanberg K. The method of moving asymptotes—a new method for structural optimization. Internat J Numer Methods Engrg 1987;24(2):359–73. http://dx.doi.org/10.1002/nme.1620240207.

[22] Lazarov BS, Sigmund O. Filters in topology optimization based on Helmholtz-type differential equations. Internat J Numer Methods Engrg 2011;86(6):765–81. http://dx.doi.org/10.1002/nme.3072.

[23] Carstensen JV, Guest JK. Projection-based two-phase minimum and maximum length scale control in topology optimization. Struct. Multidiscip. Optim. 2018;58(5):1845–60. http://dx.doi.org/10.1007/s00158-018-2066-4.

[24] Sigmund O, Maute K. Topology optimization approaches. Struct Multidiscip Optim 2013;48(6):1031–55. http://dx.doi.org/10.1007/s00158-013-0978-6.